Investigation of activation cross-section data of proton induced nuclear reactions on rhenium

F. Ditrói[a,*], F. Tárkányi[a], S. Takács[a], A. Hermanne[b], H. Yamazaki[c], M. Baba[c], A. Mohammadi[c], A.V. Ignatyuk[d]

[a]*Institute of Nuclear Research of the Hungarian Academy of Sciences (ATOMKI), Debrecen, Hungary*
[b]*Cyclotron Laboratory, Vrije Universiteit Brussel (VUB), Brussels, Belgium*
[c]*Cyclotron Radioisotope Center (CYRIC), Tohoku University, Sendai, Japan*
[d]*Institute of Physics and Power Engineering (IPPE), Obninsk, Russia*

Abstract

In the frame of systematic investigations of activation cross-section data for different applications the excitation functions of ^{nat}Re(p,x)^{185}Os, ^{183m}Os, ^{183g}Os, ^{182}Os, ^{181m}Os, ^{186g}Re, ^{184m}Re, ^{184g}Re, ^{183}Re, ^{182m}Re, ^{182g}Re and ^{181g}Re reactions were measured up to 70 MeV. The data for the ^{nat}Re(p,x)^{183m}Os, ^{183g}Os, ^{182}Os, ^{181g}Os, ^{186g}Re, ^{184m}Re,^{182m}Re, ^{182g}Re, ^{181}Re reactions are reported for the first time. Activation method, stacked foil irradiation technique and γ-spectroscopy for activity detection were used. The experimental data were compared with predictions of three theoretical codes. From the measured cross-section thick target integral yields were also calculated and presented.

Keywords: Re targets, proton induced reactions, experimental cross-sections, model calculations, Os and Re radioisotopes

1. Introduction

To meet requirements for different practical applications we started to establish an experimental activation database some years ago by performing new experiments and a systematical survey of existing data of proton induced cross-sections up to 100 MeV and deuteron induced cross-sections up to 50 MeV (Tárkányi, 2011; Tárkányi et al., 2011). The proton activation data for rhenium (Re) are relevant for accelerator and target technology (rhenium-tungsten alloy target in Fermilab, Austron, etc.); for medical radioisotope production; for producing radioactive ion beams (RIB); for controlled fusion experiments and reactors (ITER, DEMO, etc.); for space applications; for thin layer activation (TLA); etc. Rhenium is a very heavy (atomic mass: 186.207 g/mol) and dense metal (ρ = 21.02 g/cm^3), with high melting point (3180.0 ^{o}C) and it is resistant to heat, wear and corrosion. Presently it is mostly used as an additive in super-alloys for aviation technology. The technical and medical applications are discussed in more detail in recently submitted work on activation data of deuteron induced reactions on rhenium (Ditri et al., 2012). Earlier literature contains only few experimental data on proton activation of rhenium. Armini and Bunker investigated the long-lived isotope production cross-sections from proton bombardment of rhenium, from 15 to 160 MeV, ^{185}Os, ^{183}Re(cum), ^{184g}Re (Armini and Bunker, 1975). Dmitriev measured the thick target yield data for production of ^{185}Os at 22 MeV in (Dmitriev and Molin, 1981) and (Dmitriev, 1983), Ignatyuk (Ignatyuk et al., 1984) and Okolovich (Okolovich et al., 1974) investigated the properties of rhenium in the frame of a study on fissibility of sub-actinide nuclei by protons . Results for estimation of production cross-sections on rhenium by protons through model calculations were produced by ALICE-IPPE code (Dityuk et al., 1998) in the MENDL-2p (Shubin et al., 1998) database, with TALYS code (Koning et al., 2007) in TENDL-2011 (Koning and Rochman, 2011) library and recently Maiti (Maiti, 2011) published calculations for different light ion induced reactions for production of rhenium isotopes.

2. Experiment and data evaluation

The excitation functions were measured up to 70 MeV incident energy via the activation technique by bombarding stacked Mo(52.5%)Re(47.5%) alloy foils (©Goodfellow >99.98%, thickness 50 μm) targets with a low intensity proton beam at the AVF-930 cyclotron

*Corresponding author: ditroi@atomki.hu

of the Cyclotron Laboratory (CYRIC) of the Tohoku University, Sendai, Japan and with 37 MeV protons at the CGR-560 cyclotron of the Vrije Universiteit Brussel (VUB), Brussels, Belgium. The procedures for irradiation, activity measurement and the data evaluation method (including estimation of uncertainties) were similar as described in several earlier works published by authors from the research groups in Debrecen, Brussels and Sendai. Here we summarize only the most salient features of the experimental and data evaluation technique pertaining to the present work (Ditrói et al., 2012). Special care was taken in preparation of uniform targets with known thickness, in determination of the energy and of the intensity of the bombarding beam along the target stack and in determination of the activities of the samples. The target foils were purchased from the Goodfellow company with guaranteed thickness tolerances. The sizes and weights of the whole metal sheets were measured and the average thickness was calculated. After cutting them into proper sizes they were measured again and the uniformity was verified by comparing them to the average values. In case of the CYRYC irradiation the MoRe target foils were stacked together with other target foils (CuMnNi alloy, ScO, NdO) and with 100 μm thick Al foils used to monitor the beam parameters. The irradiation of the targets was performed in He gas atmosphere in a water cooled target holder. The target stack was irradiated with a collimated, 70 MeV incident energy proton beam for 20 min at about 25 nA. The radioactivity of each sample and monitor foil was measured non-destructively by HPGe γ-spectrometry. Counting was started about 40 hours after the end of the bombardment (EOB). For the VUB irradiation the stack contained 50 μm MoRe target foils and 12 μm Ti monitor foils. The stack was irradiated in a Faraday-cup like target holder, equipped with a collimator (effective beam diameter on target is 5 μm) and a secondary electron suppressor. Irradiation took place with a collimated, 36 MeV incident energy proton beam for 30 min at a constant beam current of 130 nA. Counting of the samples started about 6 hours after EOB. The decay data were taken from NUDAT (Kinsey et al., 1997) (see Table 1), the reaction Q-values from Pritychenko and A. Sonzogni (Pritychenko and Sonzogni, 2003) the standard cross-section data for the used monitor reactions ^{nat}Al(p,x)^{22,24}Na and ^{nat}Ti(p,x)^{48}V were taken from Tárkányi (Tárkányi et al., 2001) updated in 2006 (IAEA, 2006). The energy degradation along the stack was determined via calculation (Andersen and Ziegler, 1977) and corrected on the basis of the simultaneously measured monitor reactions by the method described by Trknyi (Tárkányi et al., 1991). The ex-
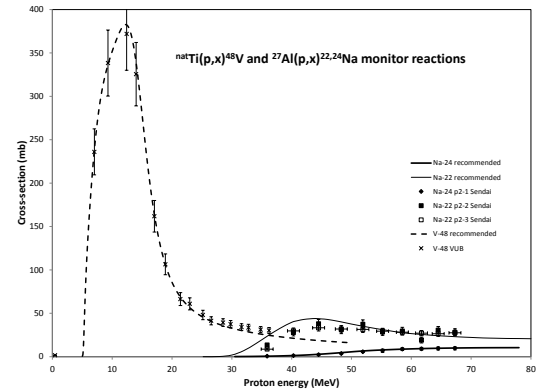

Figure 1: Application of ^{nat}T(p,x)^{48}V and ^{27}Al(p,x)^{22,24}Na monitor reactions for determination of proton beam energy and intensity

citation functions were hence determined in an accurate way relative to the simultaneously re-measured monitor reactions. (see Fig. 1).

As naturally occurring rhenium is composed of two stable isotopes ^{185}Re (37.40%), and ^{187}Re (62.60%), so called elemental cross-sections were determined supposing the rhenium is composed of only one single isotope. The resulting uncertainty on the cross-sections contain the individual uncertainties of the processes contributing linearly to the final result and are calculated accordingly to the well-accepted summation rules (of-Weights-and Measures, 1993). Quadratic summation of the uncertainties of the contributing parameters results an absolute error of 8.5% (target thickness (2%), detector efficiency (5%), physical decay data (5%), integrated beam current (2%), counting statistics (2%)). The uncertainties of the non-linear processes like half-life, irradiation time and measuring time were neglected. The uncertainty on the median energy in the targets was estimated from the uncertainty of the energy of the bombarding beam (starting from 0.3 MeV by the incident energy), the uncertainty in the thickness and uniformity of all foils, the beam straggling taking into account the cumulative effects.

3. Tehoretical calculations

The measured excitation functions were compared to theoretical effective cross-sections calculated by means of three different computer codes. For the precompound model codes ALICE-IPPE (Dityuk et al., 1998) and EMPIRE-II (Herman et al., 2007) the pa-

rameters for the optical model, level densities and pre-equilibrium contributions were taken as described in (Belgya et al., 2005). The third set of values in figures represents data in the TENDL 2011 online library (Koning and Rochman, 2011) calculated with the 1.4 version of TALYS. Results of ALICE-IPPE for excited states were obtained by applying the isomeric ratios derived from the EMPIRE code to the total cross-sections from ALICE. For each activation product reaction cross-sections on the individual target isotopes were calculated up to 100 MeV proton energy and a weighted summation (weighting factor is abundance of natural occurrence) was made to obtain the production cross-section. In case of ^{185}Os, ^{183}Re and ^{184g}Re the TENDL 2011 data (Koning and Rochman, 2011) are presented up to 200 MeV for comparison with the earlier experimental data of Armini (Armini and Bunker, 1975).

4. Results and discussions

4.1. Cross-sections

By irradiating rhenium with 70 MeV protons, many radioisotopes of different elements are produced in significant amounts. Among the radionuclides formed, unfortunately many have decay characteristics (very short or too long half-life or no γ-lines) resulting in activities below the detection limits in our measuring circumstances (long waiting time in the high energy irradiation). In the 2 experiments only radioisotopes of Os and Re were identified with proper reliability. The measured experimental cross-section data are shown in Figs 2-17 together with the theoretical results. The contributions of the two stable target isotopes (^{185}Re and ^{187}Re) are well separated. The numerical values essential for further evaluation are collected in Tables 2-4. In the figures the results of irradiations made at different primary energies at different accelerators are marked separately. The results of the two irradiations show good agreement in the overlapping energy range.

4.1.1. Production of osmium isotopes

The radioisotopes of osmium are produced only directly by (p,xn) reactions. In our spectra we could identify the ^{185}Os, ^{183m}Os, ^{183g}Os, ^{182}Os radioisotopes. Due to the long waiting time after EOB we could not find the relatively longer-lived ^{181}Os (105 min) in the measurements after the 70 MeV irradiation.

^{nat}**Re(p,x)**^{185}**Os**

The ^{185}Os radioisotope (93.6 d) is formed by the ^{185}Re(p,n)^{185}Os and ^{187}Re(p,3n)^{185}Os reactions. The
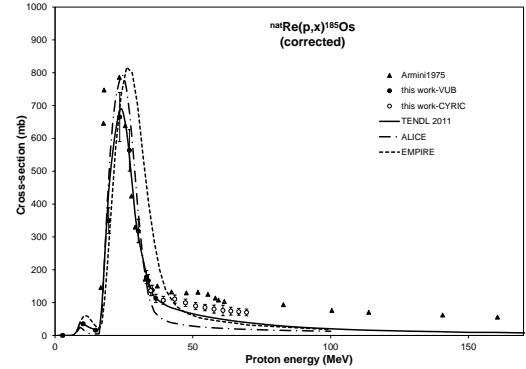

Figure 2: Experimental and theoretical excitation functions for ^{nat}Re(p,x)^{185}Os reaction

contributions of the two reactions are well separated in Fig. 2. The maximum of the (p,n) cross-section is significantly lower than that for (p,3n). Our data are in acceptable agreement with the earlier experimental data of Armini (Armini and Bunker, 1975). The TALYS and ALICE codes reproduce well the low energy part, but underestimate the high energy tail. EMPIRE predicts a significantly wider ^{187}Re(p,3n) peak than we found experimentally.

^{nat}**Re(p,x)**^{183m}**Os and** ^{nat}**Re(p,x)**^{183g}**Os** A shorter-lived excited state (T$_{1/2}$ = 9.9 h) and a longer-lived (13.0 h) ground state exist for ^{183}Os. The isomeric state has a 15% isomeric transition probability to the ground state. We present here independent results for production of ^{183m}Os (Fig. 3) and for ^{183g}Os, corrected for the isomeric decay of ^{183m}Os (Fig. 4). The shape of the theoretical predictions follows our experimental results, but the cross-section values for ^{183m}Os production are underestimated by the TENDL 2011, while for ^{183g}Os there are overestimations in all codes for the low energy maximum. At the high energy maximum the agreement is better. The width of the peaks of the calculated ^{185}Re(p,3n), ^{187}Re(p,5n) contributions in the case of EMPIRE is larger in both cases.

^{nat}**Re(p,x)**^{182}**Os** The experimental and theoretical data for production of the ^{182}Os (21.84 h) are shown in Fig. 5. There is a good agreement between the experimental data and the TENDL 2011 results in the whole investigated energy range. ALICE-IPPE overestimates peak values by 50% for (p,4n) but agrees well for the (p,6n). The broader peaks and an energy shift of about
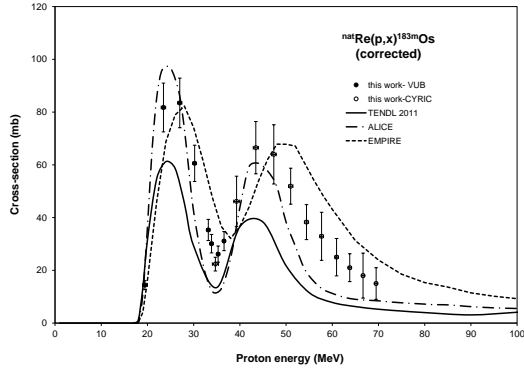
Figure 3: Experimental and theoretical excitation functions for ^{nat}Re(p,x)^{183m}Os reaction
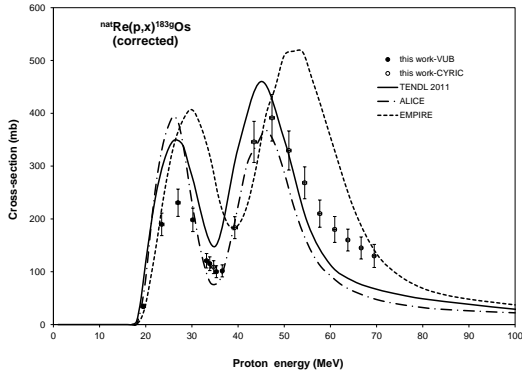

Figure 4: Experimental and theoretical excitation functions for ^{nat}Re(p,x)^{183g}Os reaction
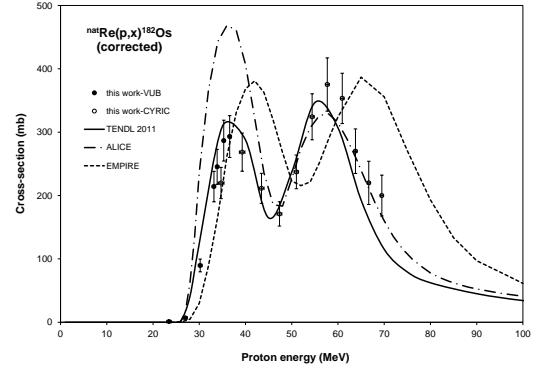

Figure 5: Experimental and theoretical excitation functions for ^{nat}Re(p,x)^{182}Os reaction

10 MeV for EMPIRE predictions can be observed.

^{nat}**Re(p,x)**^{181g}**Os** Our two experimental data points and the theoretical data for production of the ^{181g}Os (105 min) are shown in Fig. 6. It has no isomeric decay from the short-lived excited state (2.7 min). In spite of the predictions of the theoretical calculations we could not detect ^{181g}Os in the high energy irradiation, due to its short half-life and the long cooling time. The EMPIRE results are energy shifted, compared to the predictions of the two other codes.

4.1.2. Cross-sections of residual radio-products of rhenium

The radioisotopes of Re can be formed in two routes: directly via (p,pxn) reactions and by decay of simultaneously produced progenitor radioisotopes of Os and W. The effect of the secondary neutrons via (n,γ) and (n,2n) reactions should also be taken into account, but it was negligibly small in our experiments according to measurement of produced radioisotopes behind the range of the bombarding charged particles.

^{nat}**Re(p,x)**^{186g}**Re** The ^{186g}Re (3.7183 d) is produced directly only through the ^{187}Re(p,pn) reaction and through the internal decay (IT/0.150) of the very long half-life 186mRe(2.0 10^5 a), which contribution is negligible in the present experiment. The measured experimental results for ^{186g}Re are shown in Fig. 7 in comparison with the theoretical data. The model codes predict acceptable well the experimental results (both in shape and in magnitude).

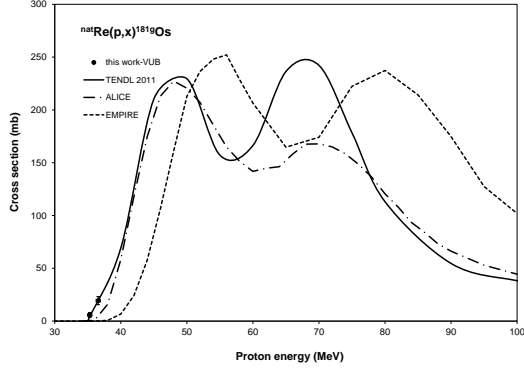^{nat}**Re(p,x)**^{184m}**Re and** ^{nat}**Re(p,x)**^{184g}**Re** The ^{184}Re ra-

4

Figure 6: Experimental and theoretical excitation functions for ^{nat}Re(p,x)^{181}Os reaction
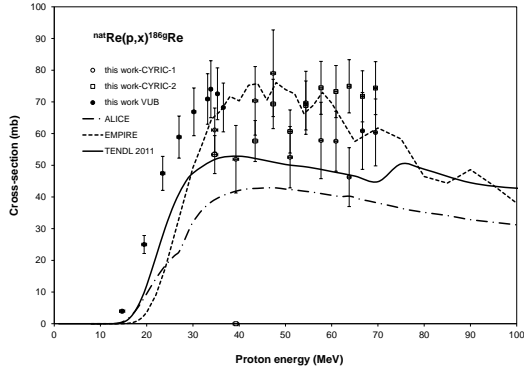

Figure 7: Experimental and theoretical excitation functions for ^{nat}Re(p,x)^{186g}Re reaction
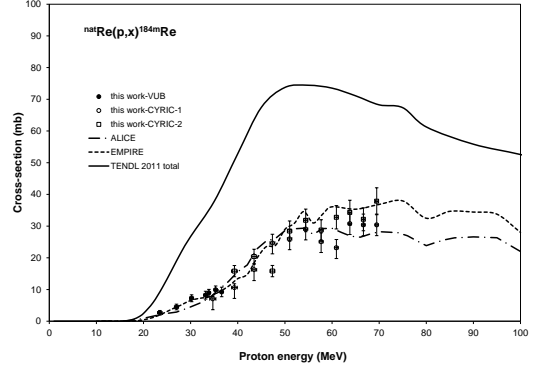

Figure 8: Experimental and theoretical excitation functions for ^{nat}Re(p,x)^{184m}Re reaction

dionuclide has a long-lived ($T_{1/2}$ =169 d) metastable state decaying for 74.5% to the 35.4 d ground state by IT. According to Fig. 8 the measured excitation function for ^{184m}Re (no clear distinction in contribution of the 2 stable target isotopes) is in good agreement with the results of ALICE and EMPIRE calculations, but it significant lower than the data in the TENDL 2011 library. We present here independent results for production of ^{184g}Re (35.4 d), which does not contain the contribution from the decay of isomeric state. For comparison also the values published by Armani (Armini and Bunker, 1975) are presented. The agreement of the experimental data and the theory in this case is much better (see Fig. 9) also for TENDL 2011 data.

^{nat}**Re(p,x)**^{183}**Re** The measured cumulative cross-sections of the ^{183}Re (70.0 d) contain contribution from the ^{185}Re(p,p2n) and ^{187}Re(p,p4n) reactions and from the ^{183m}Os (9.9 h) and ^{183g}Os (13.0 h) decay. The data were obtained from -spectra measured after a long cooling time. As it shown in Fig. 10 the theories predict the magnitude and the shape of the excitation function more or less properly.

^{nat}**Re(p,x)**^{182m}**Re and** ^{nat}**Re(p,x)**^{182g}**Re** The radionuclide 182Re has two longer-lived isomeric states, both decay independently. The higher energy, low spin isomeric state (12.7 h, 2$^+$) is produced directly and through the decay of the parent ^{182}Os (21.84 h), while ^{182g}Re (64 h, 7$^+$) is only produced directly. In Fig. 11 we present independent cross-sections for the metatable state after substracting the conributon of the parent decay. The correction was possible only for the low energy irradi-
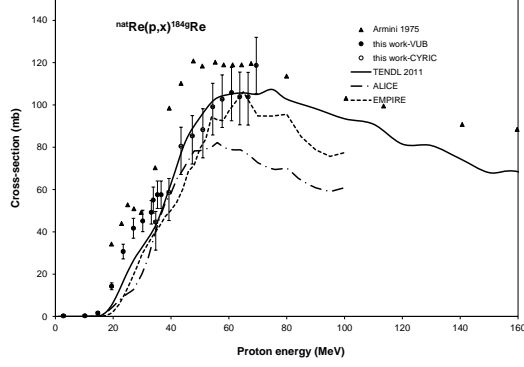
Figure 9: Experimental and theoretical excitation functions for ^{nat}Re(p,x)^{184g}Re reaction
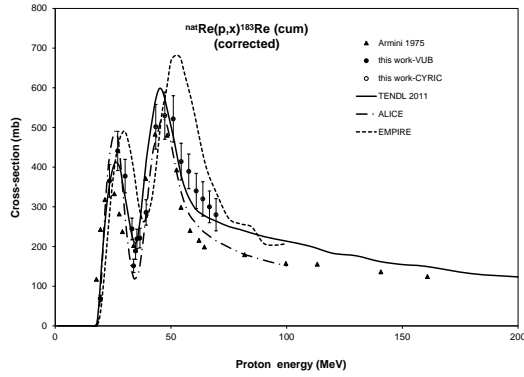

Figure 10: Experimental and theoretical excitation functions for ^{nat}Re(p,x)^{183}Re (cum) reaction
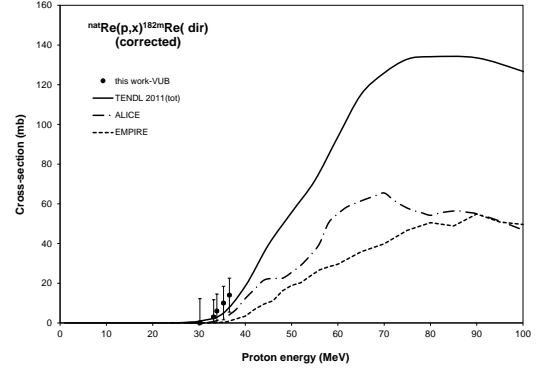
Figure 11: Experimental and theoretical excitation functions for ^{nat}Re(p,x)^{182m}Re reaction

ation and the correction is so large that the final data contains very large uncertainties. For the high energy irradiation the first measurerement started only after 3 half-life of ^{182m}Re, resulting in very low count rates of this radioisotope. The new experimental data for production of the ^{182g}Re are shown in Fig. 12.

^{nat}**Re(p,x)**^{181}**Re** The measured cumulative cross-sections contain the full contribution from decay of both isomeric states of the parent ^{181}Os (half-lives are 105 min and 2.7 min respectively). The agreement with the results of the theoretical codes is acceptably good.

4.2. Integral yields

On the basis of the measured experimental data we calculated the integral yields for the proton induced reactions on ^{nat}Re (see Fig. 14 and Fig. 15). Only one experimental work reporting on thick target yield data was found in the literature for production of ^{185}Os at 22 MeV (Dmitriev and Molin, 1981), which corresponds well to our new results.

5. Summary and conclusion

Activation cross-sections of proton induced nuclear reactions on rhenium were measured for 12 reaction products up to 70 MeV, out of them data for 7 reactions are presented here for the first time. Model calculations were done by using the EMPIRE and Alice-IPPE codes. The results were also compared with the data of the TALYS based TENDL 2011 online library. The predictions of theoretical calculations could be considered only moderately successful, especially for isomeric

Figure 12: Experimental and theoretical excitation functions for ^{nat}Re(p,x)^{182g}Re reaction

Figure 14: Integral yields for production of some Os radioisotopes

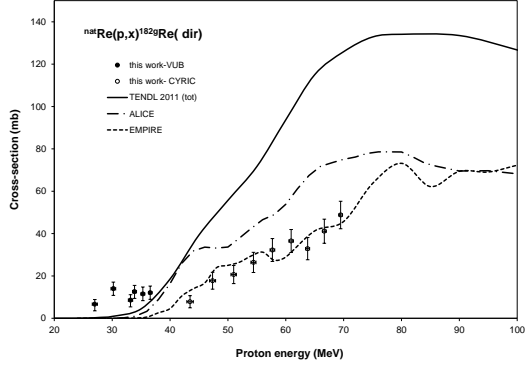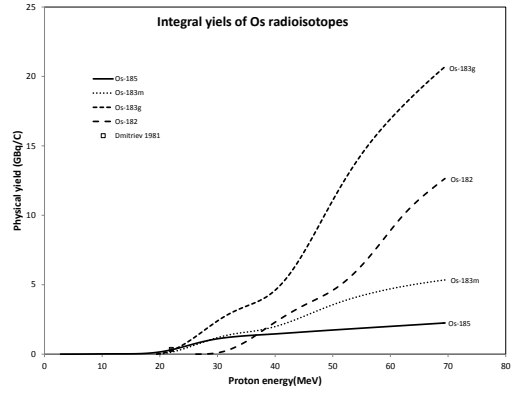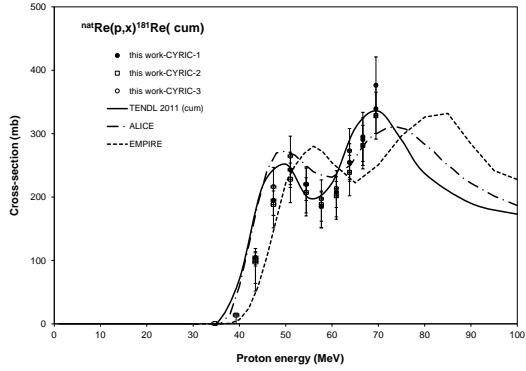

Figure 13: Experimental and theoretical excitation functions for ^{nat}Re(p,x)^{181m}Re reaction
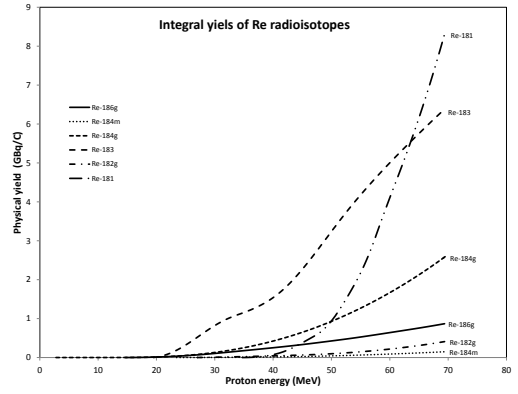

Figure 15: Integral yields for production of some Re radioisotopes

states. The obtained experimental data provide a basis for model calculations and for different applications.

6. Acknowledgements

Table 1: Decay characteristics of the investigated activation products and Q-values of contributing reactions

Nuclide	Half-life	E_γ(keV)	I_γ(%)	Contributing reaction	Q-value (keV)
^{185}Os ε: 100 %	93.6 d	646.116 717.424 874.813 880.523	78 3.94 6.29 5.17	^{185}Re(p,n) ^{187}Re(p,3n)	-1795.144 -15331.34
^{183m}Os IT: 15% ε: 85% 170.715 keV	9.9 h	1034.86 1101.92 1107.9	6.02 49.0 22.4	^{185}Re(p,3n) ^{187}Re(p,5n)	-17084.4 -30620.6
^{183g}Os ε: 100 %	13.0 h	114.47 236.367 381.763 851.48	20.6 3.41 89.6 4.56	^{185}Re(p,3n) ^{187}Re(p,5n)	-17084.4 -30620.6
^{182}Os ε: 100%	21.84 h	130.80 180.20 263.29	3.30 34.1 6.76	^{185}Re(p,4n) ^{187}Re(p,6n)	-24209.4 -37745.6
^{181g}Os	105 m	238.75 242.91 787.6 826.77 831.62	44 6.1 5.3 20 7.7	^{185}Re(p,5n) ^{187}Re(p,7n)	-33336.8 -46873.0
^{186g}Re β^-: 92.53% ε: 7.47%	3.7183 d	137.157	9.47	^{187}Re(p,pn)	-7356.84
^{184m}Re IT: 74.5% ε: 25.5% 188.0463 keV	169 d	104.7395 161.269 216.547 252.845 318.008	13.6 6.56 9.5 10.8 5.81	^{185}Re(p,pn) ^{187}Re(p,p3n)	-7666.84 -21203.03
^{184g}Re ε: 100%	35.4 d	111.2174 792.067 894.760 903.282	17.2 37.7 15.7 38.1	^{185}Re(p,pn) ^{187}Re(p,p3n)	-7666.84 -21203.03
^{183}Re	70.0 d ε: 100	162.3266 291.7282	23.3 3.05	^{185}Re(p,p2n) ^{187}Re(p,p4n) ^{183}Os decay	-14153.76 -27689.95
^{182m}Re ε: 100% 0+X keV	12.7 h	100.12 152.43 229. 32 470.26* 894.85* 1121.4 1189.2 1221.5 1231.2	14.4 7.0 2.6 2.02 2.11 32.0 15.1 25.0 1.32	^{185}Re(p,p3n) ^{187}Re(p,p5n)	-22589.0 -36125.0
^{182g}Re ε: 100%	64.0 h	100.10 130.81* 169.15* 191.39* 229.32 286.56* 351.07* 1076.2* 1121.3 1189.0 1221.4 1231.0 1427.3*	16.5 7.5 11.4 6.7 25.8 7.1 10.3 10.6 22.1 9.1 17.5 14.9 9.8	^{185}Re(p,p3n) ^{187}Re(p,p5n)	-22589.0 -36125.0
^{181}Re ε: 100%	19.9 h	360.7 365.5	20 56	^{185}Re(p,p4n) ^{187}Re(p,p6n)	-29596.0 -43132.2

The Q-values refer to formation of the ground state and are obtained from (Pritychenko and Sonzogni, 2003).
When complex particles are emitted instead of individual protons and neutrons the Q-values have to be decreased by the respective binding energies of the compound particles: np-d, +2.2 MeV; 2np-t, +8.48 MeV; n2p-^{3}He, +7.72 MeV; 2n2p-α, +28.30 MeV The independent γ-lines are marked with "*"

Table 2: Measured cross-sections for production of the ^{185}Os, ^{183m}Os, ^{183g}Os, ^{182}Os and ^{181g}Os radionuclides

Energy (MeV)	ΔE	Cross-section Δδ (mbarn)									
		^{185}Os		^{183m}Os		^{183g}Os		^{182}Os		^{181g}Os	
VUB											
36.6	0.3	112.8	12.7	31.1	3.6	101.6	11.4	293.1	33.0	19.3	3.8
35.3	0.3	137.6	15.5	26.1	3.1	100.1	11.3	286.7	32.2	5.7	2.4
33.9	0.3	166.3	18.7	30.1	3.5	115.2	13.0	245.4	27.6		
33.2	0.4	177.7	20.0	35.3	4.0	120.8	13.6	214.1	24.1		
30.2	0.4	317.9	35.7	60.6	6.9	198.2	22.3	89.6	10.1		
27.0	0.4	563.6	63.3	83.5	9.4	230.7	25.9	6.9	1.1		
23.5	0.5	665.2	74.7	81.7	9.3	189.6	21.3	1.0	1.3		
19.5	0.5	349.6	39.2	14.4	1.7	34.5	3.9				
14.7	0.6	15.7	1.8								
10.2	0.6	35.4	4.0								
2.8	0.6	0.1	0.0								
CYRIC											
69.5	0.3	70.0	10.3	15.0	6.0	130.0	21.9	200.0	32.3		
66.7	0.3	72.0	10.3	18.0	8.5	145.0	20.8	220.0	34.2		
63.8	0.3	74.0	12.1	21.0	5.3	160.0	20.7	270.0	35.2		
60.9	0.4	76.0	15.9	25.0	7.1	180.0	24.5	353.4	39.7		
57.7	0.4	80.0	12.2	32.9	9.1	210.0	25.8	375.2	42.1		
54.4	0.4	84.8	9.7	38.3	6.6	268.3	30.2	324.3	36.4		
51.0	0.5	89.7	10.3	51.9	6.8	329.5	37.0	237.3	26.6		
47.4	0.5	99.5	11.3	64.0	11.2	391.3	44.1	171.0	19.2		
43.5	0.6	110.6	12.5	66.5	9.9	345.8	38.9	211.4	23.7		
39.3	0.6	106.9	12.1	46.1	9.6	183.5	20.8	268.5	30.1		
34.7	0.6	136.5	15.5	22.4	2.6	108.7	12.2	219.8	24.7		

Table 3: Measured cross-sections for production of the ^{186}Re, ^{184m}Re, ^{184g}Re, ^{183}Re, ^{182m}Re, ^{182g}Re and ^{181}Re radionuclides

Energy (MeV)	ΔE	Cross-sections Δδ (mbarn)													
		^{186g}Re		^{184m}Re		^{184g}Re		^{183}Re		^{182m}Re		^{182g}Re		^{181}Re	
VUB															
36.6	0.30	68.2	7.7	9.2	1.5	57.5	6.5	221.2	25.0	14.0	9.1	12.1	3.2		
35.3	0.32	72.5	8.2	9.9	1.2	57.6	6.5	219.2	24.6	10.0	10.6	11.5	3.3		
33.9	0.35	74.0	9.0	9.0	1.1	55.0	6.2	151.3	17.0	6.0	9.2	12.6	3.0		
33.2	0.38	70.9	8.0	8.2	1.2	49.2	5.6	244.3	27.5	3.0	6.1	8.5	2.6		
30.2	0.41	66.9	7.5	7.3	1.1	45.2	5.1	377.3	42.4			14.0	3.1		
27.0	0.44	58.9	6.6	4.5	0.9	41.7	4.7	440.7	49.5			6.7	2.2		
23.5	0.48	47.5	5.4	2.7	0.7	30.7	3.5	365.3	41.1						
19.5	0.51	25.0	2.8			14.3	1.6	69.0	7.8						
14.7	0.56	4.0	0.5			1.6	0.2								
10.2	0.60					0.3	0.1								
2.8	0.65					0.3	0.1								
CYRIC-1															
69.5	0.30	60.4	10.5	30.4	3.4	118.7	13.3	280.0	40.7			48.8	6.5	339.3	39.0
66.7	0.32	60.9	12.1	30.4	3.4	103.8	11.7	300.0	40.0			41.1	5.7	290.7	34.4
63.8	0.35	46.3	9.3	30.8	3.5	103.9	11.7	320.0	43.3			32.9	5.3	254.6	29.6
60.9	0.38	57.6	9.5	23.2	2.6	105.9	11.9	340.0	44.5			36.5	5.4	207.7	24.3
57.7	0.41	57.8	12.1	25.1	2.8	102.7	11.5	389.3	43.7			32.2	5.4	185.0	23.0
54.4	0.44	69.7	10.0	29.1	3.3	99.1	11.1	413.9	46.5			26.4	4.7	220.2	25.6
51.0	0.48	52.5	9.7	26.0	2.9	88.3	9.9	521.6	58.5			20.7	4.3	242.9	27.9
47.4	0.51	79.0	13.7	24.7	2.8	85.4	9.6	529.9	59.5			17.7	4.0	194.9	24.0
43.5	0.56	70.3	10.8	16.2	1.8	80.5	9.0	440.7	56.3			7.8	2.9	104.9	13.8
39.3	0.60	51.9	10.7	10.6	1.2	58.7	6.6	285.8	32.1						
34.7	0.65	61.1	7.0	7.1	0.8	44.7	5.0	188.8	21.2						
CYRIC-2															
69.5	0.30	74.3	8.3	37.9	4.2									328.3	37.0
66.7	0.32	71.7	8.1	32.1	3.6									281.4	31.8
63.8	0.35	74.9	8.4	34.3	3.9									239.0	26.9
60.9	0.38	73.3	8.2	32.8	3.7									201.9	22.8
57.7	0.41	74.4	8.4	28.8	3.2									188.2	21.3
54.4	0.44	68.9	7.7	31.8	3.6									207.1	23.3
51.0	0.48	60.7	6.8	28.4	3.2									228.1	25.7
47.4	0.51	69.3	7.8	15.8	1.8									188.2	21.3
43.5	0.56	57.7	6.5	20.4	2.3									100.7	11.4
39.3	0.60			15.8	1.8									13.8	2.2
34.7	0.65	53.4	6.0											0.5	0.2

References

Andersen, H. H., Ziegler, J. F., 1977. Hydrogen stopping powers and ranges in all elements. The Stopping and ranges of ions in matter, Volume 3. The Stopping and ranges of ions in matter. Pergamon Press, New York.

Armini, A. J., Bunker, S. N., 1975. Long lived isotope production cross-sections from proton-bombardment of rhenium. Bulletin of the American Physical Society 20 (2), 156–156.

Belgya, T., Bersillon, O., Capote, R., Fukahori, T., Zhigang, G., Goriely, S., Herman, M., Ignatyuk, A. V., Kailas, S., Koning, A., Oblozinsky, P., Plujko, V., Young, P., 2005. Handbook for calculations of nuclear reaction data: Reference Input Parameter Library. http://www-nds.iaea.org/RIPL-2/. IAEA, Vienna.

Ditrói, F., Tárkányi, F., Takács, S., Hermanne, A., Yamazaki, H., Baba, M., Mohammadi, A., Ignatyuk, A., 2012. Activation cross-sections of deuteron induced nuclear reactions rhenium up to 40 mev. Nuclear Instruments & Methods in Physics Research Section B-Beam Interactions with Materials and Atoms Submitted.

Dityuk, A. I., Konobeyev, A. Y., Lunev, V. P., Shubin, Y. N., 1998. New version of the advanced computer code alice-ippe. Tech. rep., IAEA.

Dmitriev, P. P., 1983. Systematics of nuclear reaction yields for thick target at 22 mev proton energy. Vop. At. Nauki i Tekhn., Ser.Yadernye Konstanty 2, 57.

Dmitriev, P. P., Molin, G. A., 1981. Radioactive nuclide yields for thick target at 22 mev proton energy. Vop. At. Nauki i Tekhn., Ser.Yadernye Konstanty 44 (5), 43.

Herman, M., Capote, R., Carlson, B. V., Oblozinsky, P., Sin, M., Trkov, A., Wienke, H., Zerkin, V., 2007. Empire: Nuclear reaction model code system for data evaluation. Nuclear Data Sheets 108 (12), 2655–2715.

IAEA, 2006. Excitation functions of medically important radioisotopes.

Ignatyuk, A. V., Itkis, M. G., Kamenev, I. A., Muigin, S. I., Okolovich, V. N., Smirenkin, G. N., 1984. Study of the fissility of preactinide nuclei by protons and alpha-particles. Soviet Journal of Nuclear Physics-Ussr 40 (3), 400–407.

Kinsey, R. R., Dunford, C. L., Tuli, J. K., Burrows, T. W., 1997. NUDAT 2.6. Vol. 2. Springer Hungarica Ltd, Budapest, p. 657.

Koning, A. J., Hilaire, S., Duijvestijn, M. C., 2007. Talys-1.0.

Koning, A. J., Rochman, D., 2011. Talys-based evaluated nuclear data library version 4.

Maiti, M., 2011. Probable nuclear reactions to produce proton rich rhenium radionuclides. Journal of Radioanalytical and Nuclear Chemistry 290 (1), 11–16.

of-Weights-and Measures, I.-B., 1993. Guide to the expression of uncertainty in measurement, 1st Edition. International Organization for Standardization, Genve, Switzerland.

Okolovich, V. N., Zhukova, O. A., Itkis, M. G., Mulgin, S. I., 1974. Fission of some subactinide nuclei in the (p,f) reaction. Tech. rep., Rept. Inst. Nucl.Phys., Alma-Ata, No. 112.

Pritychenko, B., Sonzogni, A., 2003. Q-value calculator.

Shubin, Y. N., Lunev, V. P., Konobeyev, A. Y., Dityuk, A. I., 1998. Mendl-2p protonreaction data library for nuclear activation (medium energy nuclear data library). Tech. rep., IAEA.

Tárkányi, F., 2011. Contribution to the experimental activation cross section database of proton and deuteron induced reactions. Tech. rep., IAEA.

Tárkányi, F., Hermanne, A., Ditrói, F., Takács, S., Király, B., Csikai, G., Baba, M., Yamazaki, H., Uddin, M. S., Ignatyuk, A. V., Qaim, S. M., 25-28 Oct., 2010 2011. Systematic study of activation cross-sections of deuteron induced reactions used in accelerator applications.

Tárkányi, F., Szelecsényi, F., Takács, S., 1991. Determination of effective bombarding energies and fluxes using improved stacked-foil technique. Acta Radiologica, Supplementum 376, 72.

Tárkányi, F., Takács, S., Gul, K., Hermanne, A., Mustafa, M. G., Nortier, M., Oblozinsky, P., Qaim, S. M., Scholten, B., Shubin, Y. N., Youxiang, Z., 2001. Beam monitor reactions (chapter 4). charged particle cross-section database for medical radioisotope production: diagnostic radioisotopes and monitor reactions. Tech. rep., IAEA.